Design of a Dual-Band Planar Sleeve Monopole Antenna With the Substrate-Integrated Coaxial Line Technology

YING C. ZHENG[1], L. ZHU [2], C. NI[1], J. DING[1], K. CAO[1], AND B. LIU [2] (Member, IEEE)

[1]State Grid Yangzhou Power Supply Company, Yangzhou 225000, China

[2]College of Electronic and Information Engineering, Nanjing University of Aeronautics and Astronautics, Nanjing 211100, China

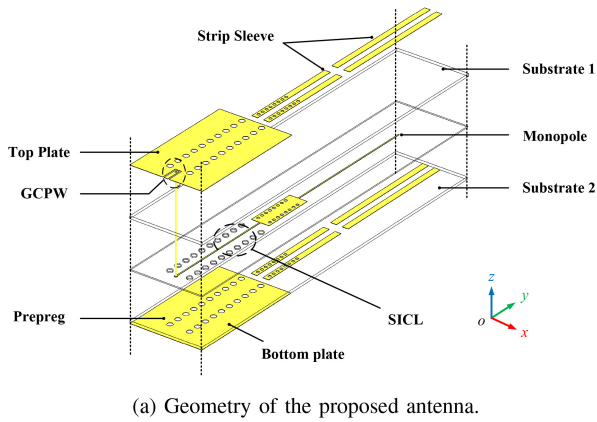CORRESPONDING AUTHOR: B. LIU (e-mail: doctice@hotmail.com)

ABSTRACT A dual-band sleeve monopole antenna with the substrate-integrated coaxial line (SICL) technology is proposed in this paper. Both the radiation structure and the feeding network are modified from the SICL structure. The antenna provides dual-band operation for LoRa (Long Range Radio) applications covering 433 MHz and 868 MHz bands. This antenna operates as a quarter-wavelength monopole with practical omnidirectional radiation performance for each band. The antenna exhibits a gain of 2.0 dBi at 433 MHz with more than 90% radiation efficiency, and a gain of 1.7 dBi at 868 MHz with more than 90% radiation efficiency. The measured −10 dB impedance bandwidths are from 393 ∼ 450 MHz and 826 ∼ 931 MHz, respectively. A good agreement is observed between the measured and the simulated results, which demonstrates that the proposed scheme can be a possible candidate for LoRa applications.

INDEX TERMS Dual-band antenna, LoRa, sleeve monopole antenna, substrate integrated coaxial line.
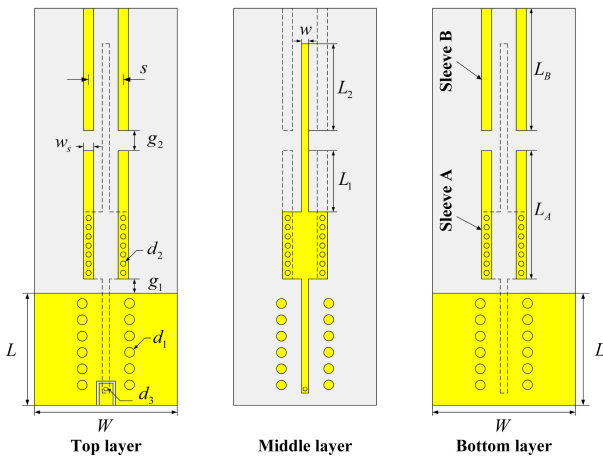
I. INTRODUCTION

WITH the rapid progress of the Internet of Things (IoT), the LoRa technology as one of the hotspot technologies attracts great interest because of its characteristics of supporting long-distance transmission while consuming low power. The current bands the LoRa standard utilized are 433 MHz and 868 MHz [1]. Sub-GHz frequency bands provide many excellent propagation characteristics, such as low power and long distance. Recently, dual-band characteristics have been preferred for network capacity expansion. Monopole is widely applied in wireless communication systems because of its simple structure, omnidirectional radiation, and good impedance matching [2], [3], [4]. Recently, in order to meet modern wireless communication systems, more research has focused on dual-band and multi-band design. A dual-band monopole design with strip sleeves was designed in [5]. A dual-band monopole antenna with a dual-sleeve structure was presented in [6]. Reference [7] proposed a wideband monopole antenna and introduced dual band-notched to achieve multi-band performance. However, these reported antennas require to be configured above a large ground plane, which is not in accordance with the development of modern communication systems on miniaturization and integration. Reference [8] presented a dual-band antenna fed by a coplanar waveguide (CPW) combining slot and F-shaped monopole. In [9], a printed double-T monopole antenna with monopoles of different sizes fed by a microstrip line was proposed. A dual-band circularly polarized monopole antenna with common-feed monopoles of different shapes and sizes was adopted in [10]. Lately, substrate-integrated coaxial line (SICL) technology has attracted much attention due to its ultra-band and non-dispersive properties [11], [12], [13], [14]. However, few monopole antennas fed by SICL have been reported yet. This paper presents a dual-band planar sleeve monopole with a dual-sleeve fed by SICL. This antenna comprises two strip-sleeve structures for dual-band operation and obtains well impedance matching at each frequency band. Moreover, this antenna can operate as a quarter-wavelength monopole and achieve omnidirectional radiation characteristics at the operating frequency bands. To the authors' knowledge, no SICL-based

(a) Geometry of the proposed antenna.

(b) Top views of different layers of the antenna

FIGURE 1. Proposed dual-band monopole antenna fed by SICL.

FIGURE 2. Electric field distribution at different frequencies.

dual-band sleeve monopole antenna has been reported yet.

A. DUAL-BAND ANTENNA DESIGN

The proposed dual-band antenna consists of a monopole surrounded by dual strip sleeves. The inner conductor of SICL is positioned between two layers of substrates and cannot be directly connected to the SMA connector, a SICL feed structure in connection with a grounded coplanar waveguide (GCPW) is designed for the convenience of measurement, as shown in Fig. 1. The inner conductor of the SICL is extended out of a monopole as the center of the sleeve antenna. The strip sleeves, with respect to the monopole's symmetry, are designed to achieve dual-band operation. In order to achieve a similar E-field distribution to the classical sleeve monopole antenna, the planar sleeves are built on the surface of upper and lower substrates. A more stable radiation pattern can be obtained with the symmetrical dual-sleeve structure.

In this design, the inner conductor of the SICL and the monopole are of the same width of w and easily impedance matched with the 50-Ω GCPW transmission line. Meanwhile, the outer conductor of SICL with the size of $W \times L$ can
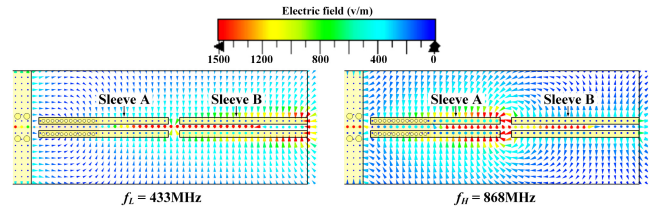
operate as the ground plane. The sleeve close to the feed is named sleeve A, and the other is named sleeve B, as shown in Fig. 1(b). The length of sleeve A is L_A, and its bottom is g_1 away from the ground. Sleeve A is connected to the widened monopole through several metalized vias at the bottom, while the top is open-ended in a length of L_1. The length of sleeve B is L_B, and there is a gap g_2 between sleeve A and B. Sleeve B exhibits open ends at both the top and the bottom. The length of the monopole surrounded by sleeve B is L_2. To simplify the design, the width of the strip-sleeve (w_s) and the offset to the center of the monopole (s) are designed to be the same, the proposed dual-sleeve structure achieves dual-band function by changing the current distribution on the inner conductor of SICL.

Since the higher frequency band operation is implemented relatively simply and is determined by sleeve A, we consider the design of sleeve A first. The length L_1 of monopole surrounded by open-ended strip-sleeve in sleeve A is

$$L_1 = \frac{1}{4} \cdot \frac{\lambda_H}{\sqrt{\varepsilon_r}} \qquad (1)$$

where λ_H is the wavelength in free space of the higher frequency (f_H) and ε_r is the dielectric constant of the substrates. The monopole is connected to the bottom of sleeve A and appears to be a short circuit at this position. With the one-quarter-wavelength monopole below, the monopole appears open-circuited at the top of sleeve A. The monopole equals to be cut at the top of sleeve A, where the E-field distribution is also affected, as shown in Fig. 2. In order to radiate at the specified frequency, the length of sleeve A needs to satisfy
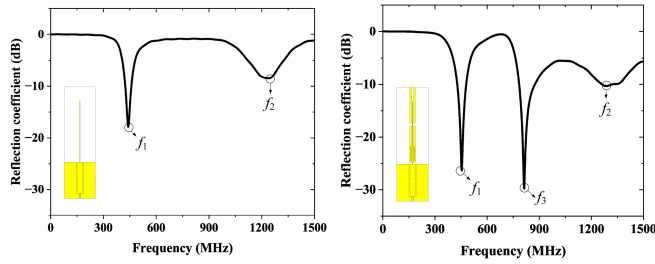
$$L_A + g_1 = \frac{\lambda_H}{4}. \qquad (2)$$

Moreover, the total width of both sleeves is much shorter than the operating-frequency wavelength, and sleeve B is located in the null direction of the radiation pattern so that the radiation is little influenced.

At the lower frequency band, the input impedance of sleeve A can be given by the transmission line theory as

$$Z_A = jZ_0 \tan\left(2\pi L_1 \sqrt{\frac{\varepsilon_r}{\lambda_L}}\right) \qquad (3)$$

where Z_0 is the characteristic impedance of the sleeve monopole and λ_L is the wavelength in free space at the lower frequency (f_L). With (1), Z_A is inductive.

(a) Original monopole fed by SICL. (b) Dual-sleeve monopole fed by SICL.

FIGURE 3. Reflection coefficients performances.

(a) Theoretically designed Performance.

(b) Effects of L.

FIGURE 4. Comparison of the reflection coefficient.

The monopole is open-circuited at the top end of sleeve B, and the input impedance is expressed as

$$Z_B = -jZ_0 \cot\left(2\pi L_2 \sqrt{\frac{\varepsilon_r}{\lambda_L}}\right). \qquad (4)$$

Similarly, Z_B is capacitive. Therefore, the dual-sleeve is equivalent to an LC series resonance circuit. The circuit is in resonance when

$$Z_A + Z_B = 0. \qquad (5)$$

The electric field between the sleeves is continuous, and the sleeves can be considered directly connected, as shown in Fig. 2. If the length of the total sleeve is satisfied

$$g_1 + L_A + g_2 + L_B = \frac{\lambda_L}{4} \qquad (6)$$

the sleeve monopole can also perform as a quarter-wavelength monopole. Substitute (3) and (4) into (5) and L_2 is given by

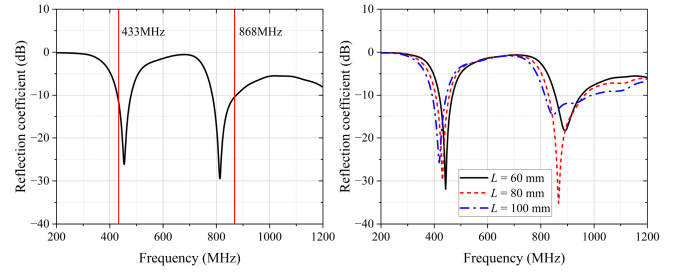$$L_2 = \frac{1}{4} \cdot \frac{\lambda_H}{\sqrt{\varepsilon_r}} - L_1. \qquad (7)$$

Therefore, the bandwidths of the proposed dual-band monopole antenna can be determined by the positions and lengths of the sleeves.

Fig. 3 illustrates the comparison of reflection coefficients between the original monopole and the proposed dual-sleeve monopole, in order to validate the accuracy of the dual-band design. It is evident that the introduction of the dual-sleeve structure results in a new resonant frequency f_3, while leaving the original quarter-wavelength monopole antenna's resonant mode unaffected.

II. SIMULATION AND EXPERIMENT RESULTS
In this design, the antenna operates at $f_L = 433$ MHz and $f_H = 868$ MHz bands for LoRa applications. It should be noted that this design is applicable for the dual-band omnidirectional antenna in various frequency bands.

This antenna consists of two 0.762 mm thick substrates (TU-883, $\varepsilon_r = 3.6$, and $tan\delta = 0.0030$) and a 0.2 mm thick prepreg (TU-883P, $\varepsilon_r = 3.6$, and $tan\delta = 0.0030$). The dimensions of the sleeves can be obtained through the

TABLE 1. Antenna performances.

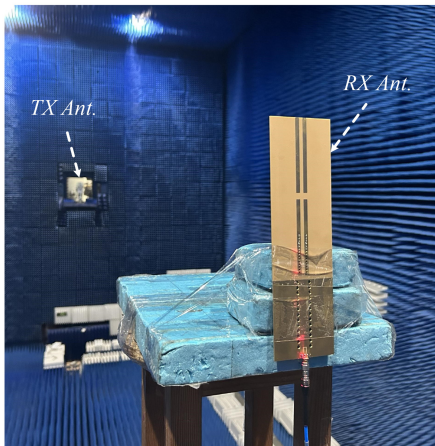| Ref.	f_L,BW (MHz,%)	f_H,BW (MHz,%)	Efficiency (%)	Gain (dBi)	Additional ground
[6]	900, 15.6	1800, 6.7	N/A	4.5, 4.8	Yes
[9]	2400, 3.5	5200, 3.8	N/A	1.8, 1.5	No
[15]	2400, 8.7	3500, 6.5	80, 70	7.5, 9.0	No
[16]	2400, 6.4	5450, 19.5	52, 87	3.8, 5.6	yes
this work	433, 13.1	868, 12.0	97, 97	0.2, 3.1	No

process of calculability in Section II. Full-wave simulations are performed to simulate and optimize the proposed design. Since the wavelength in free space (λ_H) is 345.6 mm at 868 MHz, $L_1 = 45.5$ mm, and $L_A + g_1 = 86.4$ mm. At 433 MHz, λ_L is 692.8 mm, then $L_B + g_2 = 86.8$ mm and $L_2 = 45.75$ mm. Nevertheless, the simulated reflection coefficient shown in Fig. 4(a) differs from the expected. The resonant frequencies are shifted to 454 MHz and 813 MHz, respectively. In contrast to the lower frequency, the resonance of the higher frequency is shifted down because the short-circuited monopole is equivalent to widening the monopole, and the resonance length of the monopole is shortened.

Fig. 4(b) shows the reflection coefficient concerning L, which can indicate that proper dimension L can improve impedance-matching performance and extend bandwidth. The optimized geometry dimensions of the proposed monopole antenna are follows (in mm), $L_A = 85.6$, $L_B = 84.4$, $L_1 = 35$, $L_2 = 61.2$, $L = 80$, $W = 75$, $w = 0.85$, $w_s = 4.9$, $g_1 = 5$, $g_2 = 7.5$, $d_1 = 4$, $d_2 = 2$, $d_3 = 0.5$, $s_1 = 6$, $s_2 = 3$, $s = 4.5$. The simulated performances are compared with recent reports in Table 1. It is obvious that the radiation efficiency of the proposed antenna is evidently superior to that of other antennas.

The antenna was fabricated by the standard multi-layer PCB process for experimental verification, as shown in Fig. 5(a). The antenna has a compact profile with a dimension of $270.5 \times 75 \times 1.794$ mm^3. A vector network analyzer of DEVISER-NA7662A was used to measure the reflection coefficient of the prototype. Fig. 6(a) displays the measured reflection coefficient compared with the simulated results.

(a) Prototype of the proposed dual-band monopole antenna.

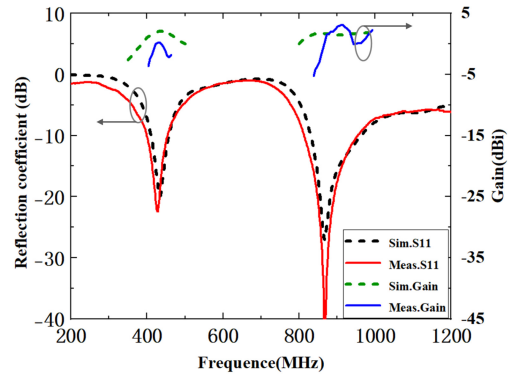(b) Measurement setup in the anechoic far-field chamber.

FIGURE 5. Prototype and test environment.

(a) Reflection coefficient.

(b) xy-plane at 433MHz

(c) xz-plane at 433MHz.

(d) xy-plane at 868MHz.

(e) xz-plane at 868MHz.

FIGURE 6. Comparison of simulated and measured results.

The measured -10 dB impedance bandwidths are $393 \sim 450$ MHz with a peak gain of 0.2 dBi, and $826 \sim 931$ MHz with a peak gain of 3.1 dBi, respectively.
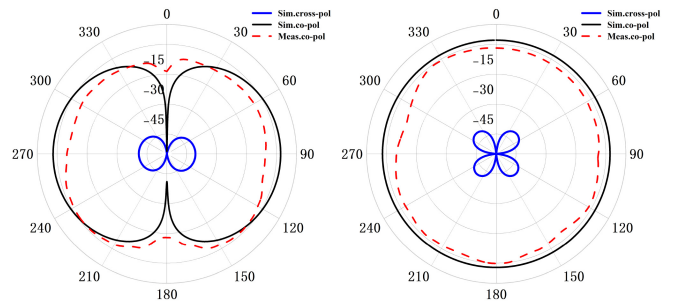
Subsequently, the gain performance and the radiation pattern were measured in a far-field anechoic chamber, as shown in Fig. 5(b). The corresponding measured gains compared with simulations of the prototype are illustrated in Fig. 6, which demonstrates that the proposed scheme radiates omnidirectionally in the xz-plane at both operating bands of 433MHz and 868MHz.

III. CONCLUSION

This paper presents a method for designing a dual-band planar monopole antenna fed by SICL technology. The enclosed SICL feed structure reduces transmission loss and makes it easy to integrate with complex circuits. The measured -10 dB impedance bandwidths are from $393 \sim 450$ MHz and $826 \sim 931$ MHz, respectively. The radiation efficiency of the proposed antenna obtained 97.1% at 433 MHz and 97.4% at 868 MHz. A good agreement between the simulated and measured results verifies the design's feasibility. The proposed antenna operates at
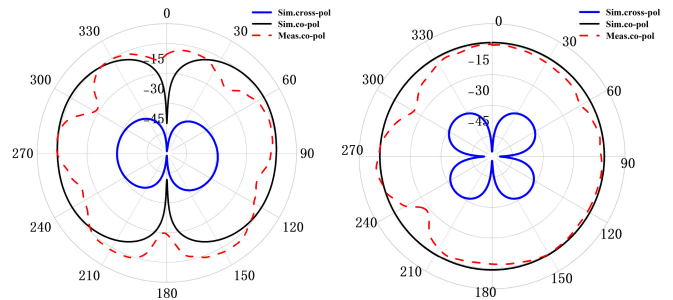
sub-GHz bands covering 433MHz and 868MHz and can be utilized for LoRa applications.

REFERENCES

[1] T. Ameloot, P. V. Torre, and H. Rogier, "LoRa base-station-to-body communication with SIMO front-to-back diversity," *IEEE Trans. Antennas Propag.*, vol. 69, no. 1, pp. 397–405, Jan. 2021.

[2] M. M. Weiner, *Monopole Antennas*. New York, NY, USA: Marcel Dekker, 2003.

[3] Z. Shen and R. H. MacPhie, "Rigorous evaluation of the input impedance of a sleeve monopole by modal-expansion method," *IEEE Trans. Antennas Propag.*, vol. 44, no. 12, pp. 1548–1591, Dec. 1996.

[4] Z. Chen, K. Hirasawa, and K. Wu, "A novel top-sleeve monopole in two parallel plates," *IEEE Trans. Antennas Propag.*, vol. 49, no. 3, pp. 438–443, Mar. 2001.

[5] M. Ali, M. Okoniewski, M. A. Stuchly, and S. S. Stuchly, "Dual-frequency strip-sleeve monopole for laptop computers," *IEEE Trans. Antennas Propag.*, vol. 47, no. 2, pp. 317–323, Feb. 1999.

[6] W. Tan and Z. Shen, "A dual-band dual-sleeve monopole antenna," *IEEE Antennas Wireless Propag. Lett*, vol. 16, pp. 2951–2954, 2017.

[7] W.-S. Lee, D.-Z. Kim, K.-J. Kim, and J.-W. Yu, "Wideband planar monopole antennas with dual band-notched characteristics," *IEEE Trans. Microw. Theory Techn.*, vol. 54, no. 6, pp. 2800–2806, Jun. 2006.

[8] X.-C. Lin and C.-C. Yu, "A dual-band CPW-fed inductive slot-monopole hybrid antenna," *IEEE Trans. Antennas Propag.*, vol. 56, no. 1, pp. 282–285, Jan. 2008.

[9] Y.-L. Kuo and K.-L. Wong, "Printed double-T monopole antenna for 2.4/5.2 GHz dual-band WLAN operations," *IEEE Trans. Antennas Propag.*, vol. 51, no. 9, pp. 2187–2192, Sep. 2003.

[10] M.-T. Tan and B.-Z. Wang, "A dual-band circularly polarized planar monopole antenna for WLAN/Wi-Fi applications," *IEEE Antennas Wireless Propag. Lett.*, vol. 15, pp. 670–673, 2016.

[11] K. Xing, B. Liu, Z. Guo, X. Wei, R. Zhao, and Y. Ma, "Backlobe and sidelobe suppression of a Q-band patch antenna array by using substrate integrated coaxial line feeding technique," *IEEE Antennas Wireless Propag. Lett.*, vol. 16, pp. 3043–3046, 2017.

[12] B. Liu et al., "A novel slot array antenna with a substrate-integrated coaxial line technique," *IEEE Antennas Wireless Propag. Lett.*, vol. 16, pp. 1743–1746, 2017.

[13] B. Liu et al., "A 45° linearly polarized slot array antenna with substrate integrated coaxial line technique," *IEEE Antennas Wireless Propag. Lett.*, vol. 17, pp. 339–342, 2018.

[14] B. Liu, Y. Ma, R. R. Zhao, W. Q. Xing, and Z. J. Guo, "A novel substrate-integrated coaxial line transverse slot array antenna," *IEEE Trans. Antennas Propag.*, vol. 67, no. 9, pp. 6187–6192, Sep. 2019.